ACADEMIC PRESS

Available online at www.sciencedirect.com

SCIENCE DIRECT®

Experimental Cell Research 287 (2003) 143–154

Experimental Cell Research

www.elsevier.com/locate/yexcr

Diacylglycerol kinase-θ is localized in the speckle domains of the nucleus

Giovanna Tabellini,[a] Roberta Bortul,[b] Spartaco Santi,[c] Massimo Riccio,[d] Giovanna Baldini,[b] Alessandra Cappellini,[a] Anna Maria Billi,[a] Ronald Berezney,[e] Alessandra Ruggeri,[a] Lucio Cocco,[a] and Alberto M. Martelli[a,c,*]

[a] *Dipartimento di Scienze Anatomiche Umane e Fisiopatologia dell' Apparato Locomotore, Sezione di Anatomia Umana, Cell Signalling Laboratory, Università di Bologna, 40126 Bologna, Italy*

[b] *Dipartimento di Morfologia Umana Normale, Università di Trieste, 34138 Trieste, Italy*

[c] *Istituto per i Trapianti d'Organo e l'Immunocitologia del C.N.R., Sezione di Bologna c/o I.O.R., 40136 Bologna, Italy*

[d] *Laboratorio di Biologia Cellulare e Microscopia Elettronica, I.O.R., 40136 Bologna, Italy*

[e] *Department of Biological Sciences, State University of New York at Buffalo, Buffalo, NY 14260, USA*

Received 12 November 2002, revised version received 28 January 2003

Abstract

It is well established that the nucleus is endowed with enzymes that are involved in lipid-dependent signal transduction pathways. Diacylglycerol (DAG) is a fundamental lipid second messenger that is produced in the nucleus. Previous reports have shown that the nucleus contains diacylglycerol kinases (DGKs), i.e., the enzymes that, by converting DAG into phosphatidic acid (PA), terminate DAG-dependent events. Here, we show, by immunofluorescence staining and confocal analysis, that DGK-θ localizes mainly to the nucleus of various cell lines, such as MDA-MB-453, MCF-7, PC12, and HeLa. Nuclear DGK-θ co-localizes with phosphatidylinositol 4,5-bisphosphate (PIP_2) in domains that correspond to nuclear speckles, as revealed by the use of an antibody to the splicing factor SC-35, a well-established marker for these structures. The spatial distribution of nuclear DGK-θ was dynamic in that it was affected by inhibition of mRNA transcription with α-amanitin. Immuno-electron microscopy analysis demonstrated that DGK-θ, PIP_2, and phosphoinositide-specific phospholipase Cβ1 (PLCβ1) associated with electron-dense particles within the nucleus that correspond to interchromatin granule clusters. Cell fractionation experiments performed in MDA-MB-453, HeLa, and PC12 cells showed a preferential association of DGK-θ with the nucleus. Western blots demonstrated that DGK-θ was enriched in the nuclear matrix fraction prepared from MDA-MB-453 cells. Immunoprecipitation experiments with an antibody to PLCβ1 revealed in MDA-MB-453 cells an association between this enzyme and both DGK-θ and phosphatidylinositol phosphate kinase Iα (PIPKIα). Our findings strengthen the contention that speckles represent a crucial site for the nuclear-based inositol lipid cycle. We may speculate that nuclear speckle-located DGK-θ, on cell stimulation with an agonist, converts to PA the DAG derived from PLCβ1-dependent PIP_2 hydrolysis.

Keywords: Inositol lipid cycle; Nucleus; Diacylglycerol; Signal transduction; Nuclear domains; Nuclear matrix

Introduction

Lipid second messengers are essential intermediates linking extracellular stimuli, via receptor activation, to the required cellular response [1,2]. These messengers are generated along very complex signaling pathways. Diacylglycerol (DAG) is a key lipid second messenger that can derive from either phosphoinositides or phosphatidylcholine [3]. DAG physiologically activates some protein kinase C (PKC) isoforms and thereby the signaling pathways downstream of PKC. The DAG-dependent PKC isozymes include conventional PKC-α, -β_I, -β_{II}, and -γ and novel PKC -δ, -ε, -η, -θ, and -μ. In contrast, atypical PKC-ζ and -ι/-λ, do not require DAG for their activation [4]. However, other molecular targets of DAG have been identified such as α- and β-chimerins, the guanine nucleotide exchange factor vav, and guanyl nucleotide-exchange factors for Ras and

* Corresponding author. Dipartimento di Scienze Anatomiche Umane e Fisiopatologia dell'Apparato Locomotore, Università di Bologna, via Irnerio 48, 40126 Bologna, Italy. Fax: +39-0512091695.

E-mail address: amartell@biocfarm.unibo.it (A.M. Martelli).

0014-4827/03/$ – see front matter © 2003 Elsevier Science (USA). All rights reserved.
doi:10.1016/S0014-4827(03)00115-0

Rap [5,6]. These findings indicate that DAG might also be involved in controlling the Ras and Rho families of proteins. In addition to cell surface receptor-mediated transmembrane signaling pathways involving phospholipid metabolism, a number of reports have convincingly demonstrated that the nucleus must also be considered as a site where biologically active lipid second messengers are generated [reviewed in 7–12]. The control of steady-state cellular levels of DAG is crucial to cellular physiology. DAG signaling must be short-lived because persistently high levels of DAG induce malignant transformation. The transforming activity of DAG has been attributed most often to persistent activation of PKC isoforms that are clearly involved in tumorigenesis [e.g., 4]. Diacylglycerol kinases (DGKs), whose activity increases on cell stimulation by a variety of agonists, metabolize DAG by converting it to phosphatidic acid (PA). Since they can attenuate local accumulation of signaling DAG, DGKs play a pivotal role in many biological responses such as cell proliferation, differentiation, survival, and apoptosis. Moreover, PA itself can function as a second messenger [13–16]. To date, nine mammalian DGK isoforms have been identified that differ in their tissue expression and structural domains [13–17]. DAG is also produced in the nucleus. The levels of nuclear DAG fluctuate during cell cycle progression, suggesting that it has important regulatory roles. Most likely, nuclear DAG serves as a chemoattractant for some isoforms of PKC that migrate to the nucleus in response to a variety of agonists [7–12,18]. Several independent laboratories have indicated that DGK isoforms are present in the nucleus where they may be involved in regulating the amount of DAG [reviewed in 19]. In some cases, the activity of nuclear DGKs has been demonstrated to be very critical for the control of cell proliferation [20–22]. When nuclear DGK isoforms were visualized by means of immunostaining or green fluorescent protein (GFP) technology, it became apparent that they were not distributed in a diffuse manner but rather concentrated in defined domains [6,20,23]. It has been proposed, but never proved, that DGK-θ is localized in the speckle domains of the nucleus [5]. The speckle domains are nuclear subcompartments enriched in small ribonucleoprotein particles and various splicing factors [reviewed in 24]. Previous results have highlighted that nuclear speckles contain elements of the phosphoinositide cycle, including various types of phosphatidylinositol phosphate kinase (PIPK) [25], phosphatidylinositol 4,5-bisphosphate (PIP_2) [26], and phosphosphoinositide 3-kinase (PI3K) [27]. In this article, we demonstrate by immunofluorescence staining and immuno-electron microscopy that also DGK-θ localizes in the nuclear speckles of different cell lines. Nuclear subfractionation experiments revealed an enrichment of DGK-θ in the nuclear matrix fraction prepared from HeLa cells. By immunoprecipitation, DGK-θ was recovered in association with both PIPKI α and PLCβ1. Our findings considerably add to the hypothesis that the speckle domains are critical subcompartments for at least some aspects of nuclear phosphoinositide metabolism.

Materials and methods

Materials

Bovine serum albumin (BSA), RNase A, fetal calf serum (FCS), horse serum (HS), normal goat serum (NGS), London Resin White (LRW), α-amanitin, peroxidase-, fluorescein isothiocyanate (FITC)- and Cy3-conjugated secondary antibodies were from Sigma (St. Louis, MO, USA). RNase-free DNase I, COMPLETE Protease Inhibitor Cocktail, and the Lumi-Light Enhanced Chemiluminescence (ECL) detection kit were from Roche Applied Science (Milan, Italy). The Protein Assay Kit (detergent compatible) was from Bio-Rad (Hercules, CA, USA). Protein G PLUS-Agarose was from Upstate Biotechnology (Lake Placid, NY, USA). Colloidal gold-conjugated secondary antibodies were from British Biocell International (Cardiff, UK). The following primary antibodies were employed in the present study: mouse monoclonals (IgG) to the splicing component SC-35 and to β-tubulin (from Sigma); mouse monoclonal (IgG) to DGK-θ and mouse monoclonal (IgM) to Nuclear Mitotic Apparatus protein (NuMA) (from BD Transduction Laboratories, Milan, Italy); mouse monoclonal (IgG) to 170-kDa topoisomerase IIα (Roche Applied Science); mouse monoclonal (IgM) to PIP_2 (from Echelon Biosciences Incorporated, Salt Lake City, UT, USA); mouse monoclonals (IgG) to histone H1 and PLCβ1 (from Upstate Biotechnology); B3, a mouse monoclonal (IgM) to a hyperphosphorylated form of the large subunit of RNA polymerase (RNA pol) II [28]; goat polyclonals to lamin B, PIPK Iα, and mouse IgM (from Santa Cruz Biotechnology, Santa Cruz, CA, USA).

Cell culture

The human mammary carcinoma cell lines MCF-7 and MDA-MB-453 were grown in RPMI-1640 containing 10% heat-inactivated FCS. Human HeLa cells were cultured in D-MEM containing 10% heat-inactivated FCS. Rat pheochromocytoma PC12 cells were grown in D-MEM containing 10% heat inactivated FCS and 5% heat-inactivated HS. For treatment with α-amanitin, HeLa cells were incubated at 37°C for 6 h with the toxin at 50 μg/ml.

Preparations of cell homogenates for Western blot analysis

Cells were washed twice in phosphate-buffered saline (PBS, pH 7.4) containing the COMPLETE Protease Inhibitor Cocktail supplemented with 1.0 mM Na_3VO_4 and 20 nM okadaic acid. Cells were lysed at $\sim 10^7$/ml in boiling electrophoresis sample buffer containing the protease inhibitor cocktail. Lysates were then briefly sonicated to shear

DNA and reduce viscosity, boiled for 5 min to solubilize protein.

Isolation of nuclei

This was accomplished as previously reported, with minor changes [29]. Briefly, cells (5×10^6) were resuspended in 10 mM Tris–HCl, pH 7.8, 10 mM NaCl, 2 mM $MgCl_2$, 10 mM β-mercaptoethanol, 1.0 mM phenylmethyl sulfonyl fluoride (PMSF), 10 μg/ml soybean trypsin inhibitor, 1 μg/ml of leupeptin and aprotinin, 1.0 mM Na_3VO_4, and 20 nM okadaic acid. They were incubated at 0°C for 20 min, then 1% Nonidet P-40 was added and the cells were allowed to swell for 10 min. Cells were sheared by four passages through a 22-gauge needle. Nuclei were recovered by centrifugation at 400*g* for 6 min and washed once in 10 mM Tris–HCl, pH 7.4, 5 mM $MgCl_2$, plus protease inhibitors as above (TM-5 buffer). Supernatant from the first centrifugation was saved and used for Western blot analysis after precipitation with 25% trichloroacetic acid. Nuclei were resuspended in TM-5 buffer at 1 mg DNA/ml.

Preparation of nuclear matrix

Nuclear matrices were isolated according to Belgrader et al. [30], with modifications. Briefly, membrane-depleted nuclei from MDA-MB-453 cells were digested with 40 IU/mg DNA of RNase-free DNase I for 30 min at 4°C. Subsequently, the chromatin-associated proteins were released by adding dropwise 2 M $(NH_4)_2SO_4$ to a final concentration of 0.6 M $(NH_4)_2SO_4$. After 15 min of incubation on ice, the nuclear matrices were pelleted at 1500 *g* for 15 min and washed once in 10 mM Tris–HCl, pH 7.4, 0.2 mM $MgCl_2$.

Immunoprecipitation

This was accomplished essentially as reported elsewhere [28] with some changes. Protein G–agarose (20 μl) were incubated with goat anti-mouse IgM as bridging antibody for 2 h at 4°C and subsequently incubated with 5 μg of anti-PIP_2 antibody for 1 h. Nuclei (from 2×10^7 MDA-MB-453 cells) were lysed for 30 min at 4°C in 5 mM Tris–HCl, pH 8.0, 10% glycerol, 1 mM EDTA, 1 mM EGTA, 0.1 mM Na_3VO_4, 1 mM PMSF, 10 μg/ml soybean trypsin inhibitor, 1 μg/ml leupeptin, and aprotinin. The suspension was passed 40 times through a 26-gauge needle, then centrifuged at 2000*g* for 15 min at 4°C. Nuclear extracts were precleared by incubation with 20 μl protein G–agarose for 1 h at 4°C, prior to the addition of either 20 μl anti-PIP_2-conjugated protein G–agarose or 5 μg anti-PLCβ1 antibody. Samples were incubated for 2 h at 4°C, then centrifuged for 5 min at 3000*g* at 4°C. Immunoprecipitates were washed four times in 20 mM Hepes–NaOH, pH 7.9, 100 mM KCl, 1.5 mM $MgCl_2$, 0.2 mM EDTA, 0.25% NP-40 and then prepared for sodium dodecyl sulfate–polyacrylamide gel electrophoresis (SDS–PAGE). Protein was quantitatively recovered from supernatants of immunoprecipitates by precipitation with 25% trichloroacetic acid.

Protein assay

This was performed according to the instruction of the manufacturer using the Bio-Rad Protein Assay (detergent compatible).

Western blot analysis

Protein separated on SDS–PAGE was transferred to nitrocellulose sheets using a semidry blotting apparatus. Sheets were saturated for 60 min at 37°C in blocking buffer, then incubated overnight at 4°C in blocking buffer (PBS supplemented with 5% NGS and 4% BSA) containing the primary antibody. After four washes in PBS containing 0.1% Tween 20, they were incubated for 30 min at room temperature with peroxidase-conjugated secondary antibody diluted 1:5000 in PBS–Tween 20, and washed as above. Bands were visualized by the ECL method. Densitometric analysis was performed on the Molecular Analyst GS670 (Bio-Rad).

Immunofluorescence staining

Cells, growing on poly-L-lysine-coated coverslips, were fixed for 30 min at room temperature with 4% freshly prepared paraformaldehyde in PBS. The coverslips were treated for 15 min with 50 mM NH_4Cl and then blocked using PBS containing 2% BSA, 0.25 gelatin, 0.2% glycine, and 0.2% Triton X-100 for 1 h at room temperature, essentially as described by Osborne et al. [26]. The primary antibodies were appropriately diluted (anti-SC-35 1:20,000; anti-PIP_2 1:25; anti-DGK-θ 1:10) in PBS with 1% BSA, 0.25% gelatin, and 0.2% Triton X-100, and incubated for 1 h at 37°C. Samples were washed with 0.2% gelatin in PBS and the fluorescent secondary antibodies (1:200 for FITC-conjugated, 1:400 for Cy3-conjugated) applied for 30 min in the same buffer as the primary antibody. FITC-conjugated anti-mouse IgG was employed to reveal SC-35 or DGK-θ, while Cy3-conjugated anti-mouse IgM was used to label PIP_2. No immunofluorescent staining was detected when primary antibodies of the IgG type were revealed by an anti-IgM or when primary antibodies of the IgM type were labeled by an anti-IgG (data not presented). RNase A (100 IU/ml for 15 min) and DNase I (200 IU/ml for 2 h) treatments were carried out postfixation in PBS containing 5 mM $MgCl_2$, 4% Tween 20 prior to blocking [27]. DNase I digestion resulted in the complete loss of DNA, as assessed by staining with Hoechst 33342 (not shown).

Confocal laser scanning microscope (CLSM) analysis

The confocal imaging was performed on a Radiance 2000 confocal laser scanning microscope (Bio-Rad), equipped with a Nikon 40×, 1.4-N.A. objective and with a krypton laser, to excite FITC (green) and Cy3 (red) fluorescence. Co-localization was evaluated on medial optical sections using LaserPix software (Bio-Rad) [29]. Briefly, the two-dimensional scatterplot diagram of each image was analyzed to evaluate the spatial co-localization of the fluorochromes. For each scatterplot diagram, pixels with highly co-localized fluorochromes, i.e., with intensity values greater than 150 gray levels (on a scale from 0 to 255) for both detectors, were selected to calculate the co-localization maps and create a binary image. Co-localization analysis (Pearson's correlation and overlap coefficient) calculated on 50 cells by LaserPix software (Bio-Rad) was performed as previously described [31,32].

Immuno-electron microscopy

A postembedding technique was used as a method for transmission immuno-electron microscopy. MDA-MB-453 cells were fixed with 4% paraformaldehyde, 0.1% glutaraldehyde in sodium phosphate buffer, pH 7.3, for 35 min at 4°C, dehydrated up to 100% ethanol, and embedded in LRW. To block nonspecific binding sites, the grids were treated with TBS buffer (20 mM Tris–HCl, pH 8.2, 225 mM NaCl containing 0.1% BSA) for 1 h at room temperature. Sections were incubated overnight at 4°C with the primary antibody (anti-SC-35 1:50; anti-PIP_2 1:25; anti-DGK-θ 1:10; B3 1:25; anti-PLCβ1 1:10). Grids were washed several times with TBS buffer and then incubated for 1 h at room temperature with the appropriate secondary antibodies diluted 1:50 in TBS. To label SC-35, DGK-θ, and PLCβ1 an anti-mouse IgG conjugated with 10-nm colloidal gold particles was employed, while to reveal PIP_2 and B3 an anti-mouse IgM conjugated with 30 nm colloidal gold particles was used. Controls consisted of samples in which the primary antibody was omitted. No colloidal gold particles were detected (not shown). Sections were examined and photographed with a JEOL-JEM 100S electron microscope.

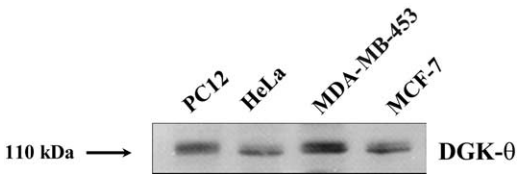

Fig. 1. Western blot analysis for DGK-θ in various cell lines. Eighty micrograms of protein from whole-cell homogenates was blotted to each lane.

Results

Expression of DKG-θ in cell lines

We first screened several cell lines for the expression of DKG-θ. Western blot analysis showed DKG-θ to be expressed in PC12, HeLa, MDA-MB-453, and MCF-7 cells (Fig. 1). The molecular weight of the protein was, as expected, about 110 kDa. In HeLa cells, however, it migrated slightly faster, around 108 kDa.

Immunofluorescence staining and CLSM analysis

We next set out a series of experiments aimed at clarifying the subnuclear localization of DKG-θ. We singly immunostained MDA-MB-453 cells for SC-35, PIP_2, and DKG-θ. As shown in Fig. 2a, CLSM analysis showed SC-35 to be located mainly in 20–40 discrete nonnucleolar domains, corresponding to speckles, as expected. Immunostaining with monoclonal antibody to PIP_2 resulted in a similar pattern, albeit in this case the foci were smaller and there was more disperse nucleoplasmic positivity (Fig. 2b). The use of a monoclonal antibody to DKG-θ gave a fluorescent signal very similar to that provided by the antibody to SC-35 (Fig. 2c). Previous results have highlighted that PIP_2 localizes to nuclear speckles of several cell types, including HeLa cells [25,26]. We wanted to confirm this finding in MDA-MB-453 cells. Double-immunofluorescence staining with antibodies to SC-35 (an IgG) and PIP_2 (an IgM) provided evidence that the two molecules co-localized at the levels of the speckles (Figs. 2d–f). These results demonstrated that the antibody to PIP_2 could be confidently used as a marker for nuclear speckles. This antibody (2C11) has previously been employed by other investigators who have thoroughly demonstrated its speci-

Fig. 2. DGK-θ localizes to discrete nuclear domains. Immunocytochemical localization of SC-35 (a), PIP_2 (b), and DGK-θ (c) in MDA-MB-453 cells. Samples were single-stained with the antibody to the protein of interest which was then revealed with FITC-conjugated anti-mouse IgG (SC-35, DGK-θ) or a Cy3-conjugated anti-mouse IgM (PIP_2). Co-localization analysis carried out in MDA-MB-453 (d–k), MCF-7 (l–o), PCl2 (p–s), and HeLa (t–w) cells. Cells were co-immunostained for either SC-35 (d) or DGK-θ (h, l, p, t) and PIP_2 (e, i, m, q, u). SC-35 and DGK-θ were revealed by FITC-conjugated anti-mouse IgG while PIP_2 was labeled by Cy3-conjugated anti-mouse IgM. Merged images (green for SC-35 or DGK-θ, and red for PIP_2) are shown in (f), (j), (n), (r), and (v). Co-localization of the fluorochromes results in a yellow color. The binary maps presented in (g), (k), (o), (s), and (w) are a more precise means to evaluate co-localization, as they only show regions in which the two signals are present together above a defined threshold of fluorescence intensity. Arrow in (j) indicates a cytoplasmic area stained only by anti-PIP_2 antibody (red). Arrow in (p) and (q) indicate a cytoplasmic area stained by both anti-DGK-θ and anti-PIP_2 antibodies. In (j), (p), and (q) the nuclear border was identified by phase contrast (not shown). Bar = 5 μm.

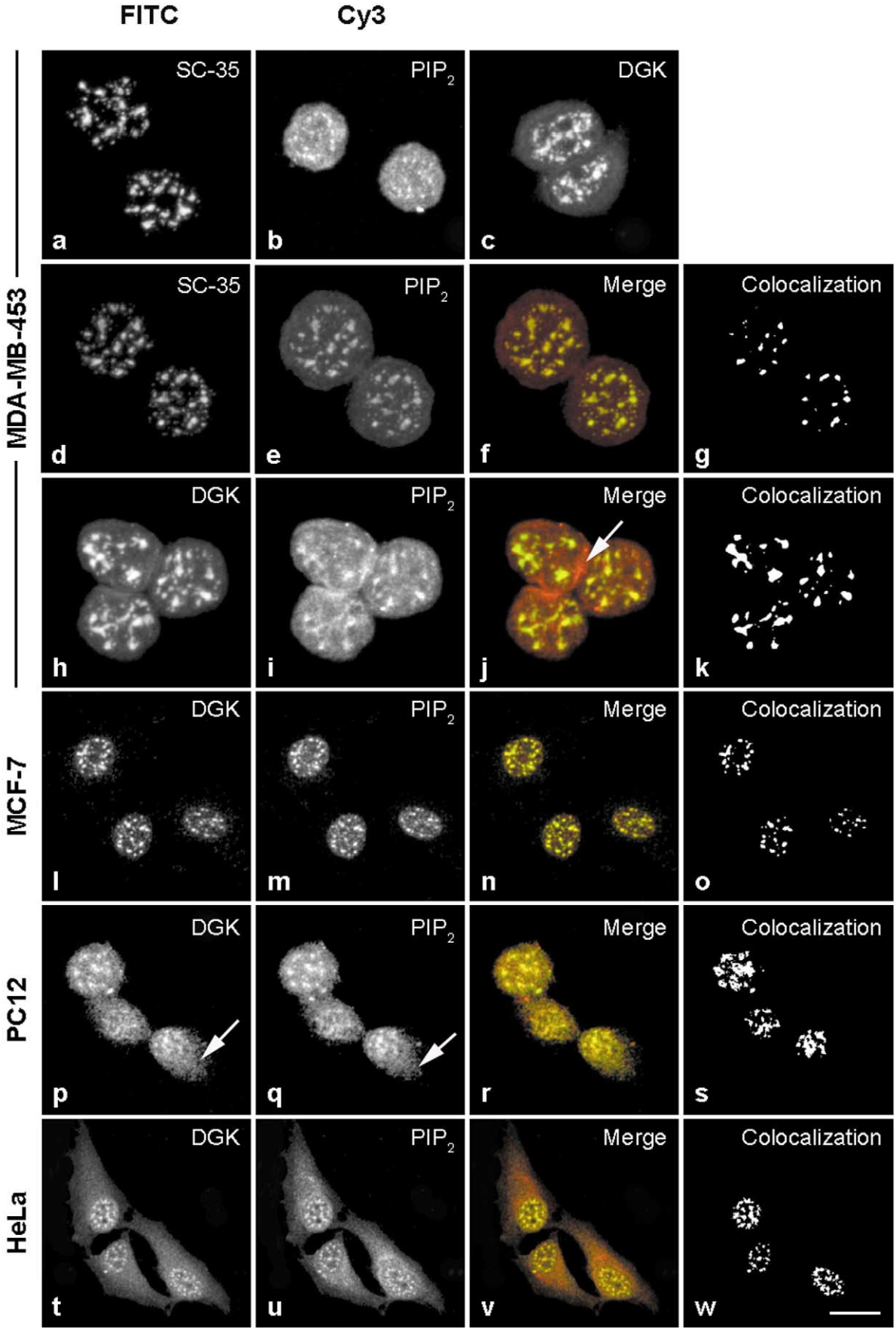
FITC
Cy3
MDA-MB-453
MCF-7
PC12
HeLa
SC-35
PIP2
DGK
Merge
Colocalization
a
b
c
d
e
f
g
h
i
j
k
l
m
n
o
p
q
r
s
t
u
v
w

Table 1
Quantification of SC-35/PIP_2 and DGK-θ/PIP_2 co-localization in different cell lines[a]

	Cell line				
	MDA-MB-453	MDA-MB-453	MCF-7	PC12	HeLa
Co-immunostaining	SC-35/PIP_2	DGK-θ/PIP_2	DGK-θ/PIP_2	DGK-θ/PIP_2	DGK-θ/PIP_2
Pearson's correlation	74 ± 9	81 ± 4	90 ± 2	97 ± 1	89 ± 8
Overlap coefficient	77 ± 8	90 ± 1	95 ± 2	97 ± 1	96 ± 2

[a] Fifty cells were analyzed for each type of co-immunostaining. The values are expressed as percentages ± SD.

ficity for PIP_2 in immunostaining experiments [26]. Double-immunofluorescence staining with antibodies to DGK-θ (an IgG) and PIP_2 showed that the two molecules co-localized at the level of nuclear foci, corresponding to speckles (Figs. 2h–j). The co-localization of DGK-θ with PIP_2 in nuclear foci was also detected in MCF-7, PC12, and HeLa cells (Figs. 2l–w). Overall, DGK-θ immunoreactivity was found mainly in the nucleus. HeLa and PC12 cells showed some DGK-θ staining in the cytoplasm, whereas in MDA-MB-453 and MCF-7 cells cytoplasmic positivity was almost undetectable. Cytoplasmic PIP_2 immunostaining was mostly seen in HeLa, MDA-MB-453, and PC12 cells.

Quantification of co-localization

We next carried out a quantitative analysis of the results provided by CLSM using both Pearson's correlation and Overlap coefficient. Pearson's correlation provides information about the similarity of shape between images without respect to the average intensity of the signals (spatial co-localization). It is a value computed to be between −1 and 1. The Overlap coefficient is simultaneously used to describe co-localization: this method does not perform any pixel averaging functions, so correlations are returned as values between 0 and 1. This method is not sensitive to intensity variations in the image analysis. This is especially important when considering issues typical of fluorescence imaging such as sample photobleaching and different settings of the detectors. As shown in Table 1, all the values for co-immunostaining of SC-35/PIP_2 and DGK-θ/PIP_2 were higher than 74%, indicating a remarkable level of co-localization.

Effect of α-amanitin on the subnuclear distribution of DGK-θ

Previous results have indicated that cell treatment with the transcriptional inhibitor α-amanitin at concentrations that specifically inhibit RNA polymerase II causes reorganization of nuclear speckle domains into fewer and/or larger foci [e.g., 33]. As shown in Fig. 3, incubation of HeLa cells for 6 h in the presence of α-amanitin caused the expected changes in SC-35 immunofluorescence staining (compare Fig. 3b with Fig. 3a). Speckles were larger and less numerous. Indeed, in control cells we counted 22 ± 5 speckles/nucleus (50 cells analyzed), whereas in response to α-amanitin the number of speckles decreased to 9 ± 3. Also, the intranuclear distribution of DGK-θ changed in response to α-amanitin (Fig. 3, compare c with d), because the foci became less numerous, even though their size did not increase as much as for SC-35 staining. In this case we counted an average of 13 ± 4 speckles/nucleus in α-amanitin-treated samples, while in control samples there were 24 ± 6. We next sought to establish whether or not the level of co-localization of SC-35 with PIP_2 and of DGK-θ with PIP_2 was maintained after treatment with α-amanitin. In untreated cells there was an almost complete co-localization of the signals (data not shown, but see Ref. [26] for SC-35/PIP_2 and Figs. 2t–y for DGK-θ/PIP_2 double immunostaining). The level of co-localization of SC-35/PIP_2 was maintained in α-amanitin-treated cells (Figs. 3e–g). In contrast, as shown in Figs. 3 h–j double-immunofluorescence labeling for DGK-θ/PIP_2 revealed that, after α-amanitin exposure, the extent of co-localization was not as high as in untreated samples (compare with Figs. 2t–v). Quantification of co-localization supported this conclusion (Table 2).

Nuclease sensitivity of DGK-θ immunostaining

It has been shown that RNA, but not DNA, is essential for the association of PIP_2 with nuclear speckles [26]. We sought to determine whether or not this was also true of DGK-θ. As shown in Fig. 4A, DNase I treatment of MDA-MB-453 cells did not affect the intranuclear distribution of DGK-θ. In contrast, RNase A treatment completely removed intranuclear immunoreactivity for DGK-θ (Fig. 4C). These results imply that RNA, but not DNA, is essential for the association of DGK-θ with speckles.

Immuno-electron microscopy analysis

The subnuclear distribution of DGK-θ in MDA-MB-453 cells was also investigated by means of immunogold staining. As presented in Fig. 5A, the SC-35 splicing factor was immunolocalized to structures corresponding to interchromatin granules and perichromatin fibrils, as previously reported [34]. These structures also contained PIP_2 (Fig. 5A), in agreement with others [25,26]. Interchromatin granule

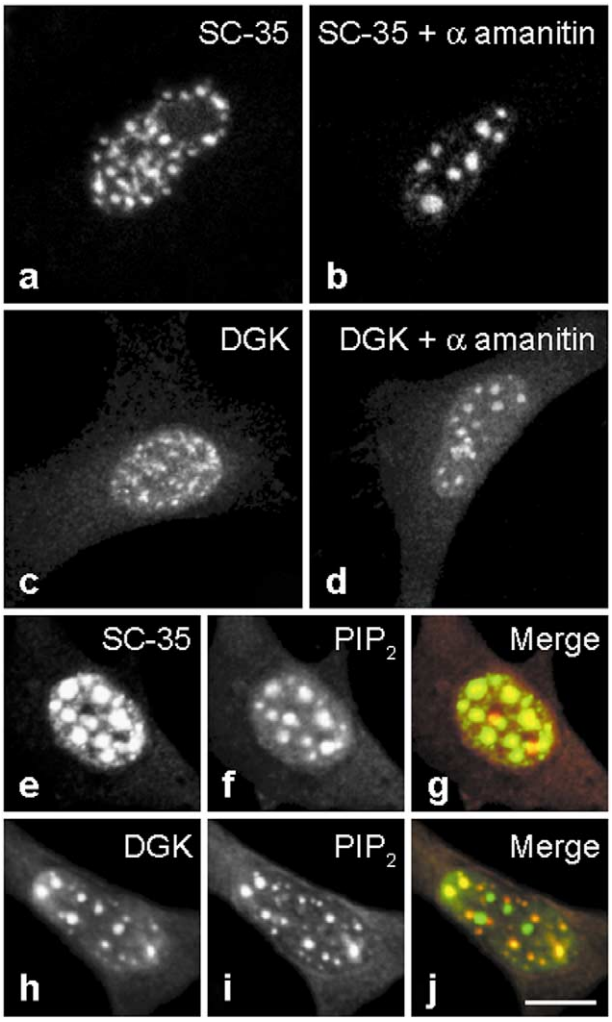

Fig. 3. Treatment with α-amanitin affects the imunofluorescence pattern of DGK-θ in HeLa cells. Immunocytochemical localization of SC-35 (a, b) and DGK-θ (c, d) in control HeLa cells (a, c) and after a 6-h incubation with 50 μg/ml α-amanitin (b, d). Double-immunofluorescence staining for SC-35/PIP_2 (e–g) and DGK-θ/PIP_2 (h–j) following a 6-h treatment with 50 μg/ml α-amanitin. SC-35 and DGK-θ were revealed by FITC-conjugated anti-mouse IgG while PIP_2 was labeled by Cy3-conjugated anti-mouse IgM. Merged images (green for SC-35 or DGK-θ, and red for PIP_2) are shown in (g) and (h). Co-localization of the fluorochromes results in a yellow colour. Bars = 5 μm.

clusters and perichromatin fibrils are thought to correspond to the 20–40 intensely stained nuclear speckles when immunofluorescence is performed with probes to a variety of splicing factors [25 and references therein]. The antibody to DGK-θ similarly labeled the interchromatin granules and perichromatin fibrils (Fig. 5B). As further proof that DGK-θ localizes to these nuclear domains, we decided to perform double-labeling experiments, using a speckle marker different from SC-35 or PIP_2. Therefore, we employed the monoclonal antibody B3 (an IgM) which recognizes a hyperphosphorylated form of RNA polymerase II associated with the speckles [28]. Indeed, as shown in Fig. 5C, both SC-35 and the antigen recognized by B3 were present in the same nuclear domain. A double-labeling experiment with antibody to DGK-θ and B3 further demonstrated that DGK-θ associated with interchromatin granules and perichromatin fibrils (Fig. 5D). Finally, in Fig. 5E we show that PLCβ1 could also be detected in these nuclear domains.

DGK-θ is enriched in the nucleus and associates with the nuclear matrix

We next analyzed the subcellular distribution of DGK-θ using Western blot. As shown in Fig. 6, in MDA-MB-453 cells the enzyme was almost entirely located in the nucleus. In contrast, in both HeLa and PC12 cells DGK-θ was predominantly, but nonexclusively nuclear, because stronger immunoreactivity was found in the postnuclear supernatant. These results were quite in agreement with the findings obtained by means of immunofluorescence staining. The use of an antibody to β-tubulin demonstrated the purity of our nuclear preparations. Since we could not obtain sufficiently pure preparations of nuclei from MCF-7 cells, these experiments were not performed in this cell line.

In Fig. 7 we demonstrate that in MDA-MB-453 cells DGK-θ was enriched in the nuclear matrix fraction which was obtained by DNase I digestion and 0.6 M $(NH_4)_2SO_4$ extraction performed on isolated nuclei to remove chromatin. The nuclear matrix fraction we prepared from these cells was enriched in 170-kDa topoisomerase IIα (an abundant component of nuclear matrix, see Ref. [35]) and NuMa (another structural component of the matrix, see Ref. [36] and references therein) but was depleted of histone H1, a well-established chromatin marker. Results obtained by means of visual inspection of the blots were corroborated by densitometric analysis (Table 3).

Table 2
Quantification of SC-35/PIP_2 and DGK-θ/PIP_2 co-localization in control (untreated) and α amanitin-treated (50 μg/ml for 6 h) HeLa cells[a]

	Co-immunostaining			
	SC-35/PIP_2	SC-35/PIP_2	DGK-θ/PIP_2	DGK-θ/PIP_2
	Control	α-Amanitin	Control	α-Amanitin
Pearson's correlation	73 ± 3	72 ± 4	95 ± 2	38 ± 2
Overlap coefficient	70 ± 5	71 ± 3	94 ± 2	42 ± 3

[a] Fifty cells were analyzed for each type of co-immunostaining. The values are expressed as percentages ± SD.

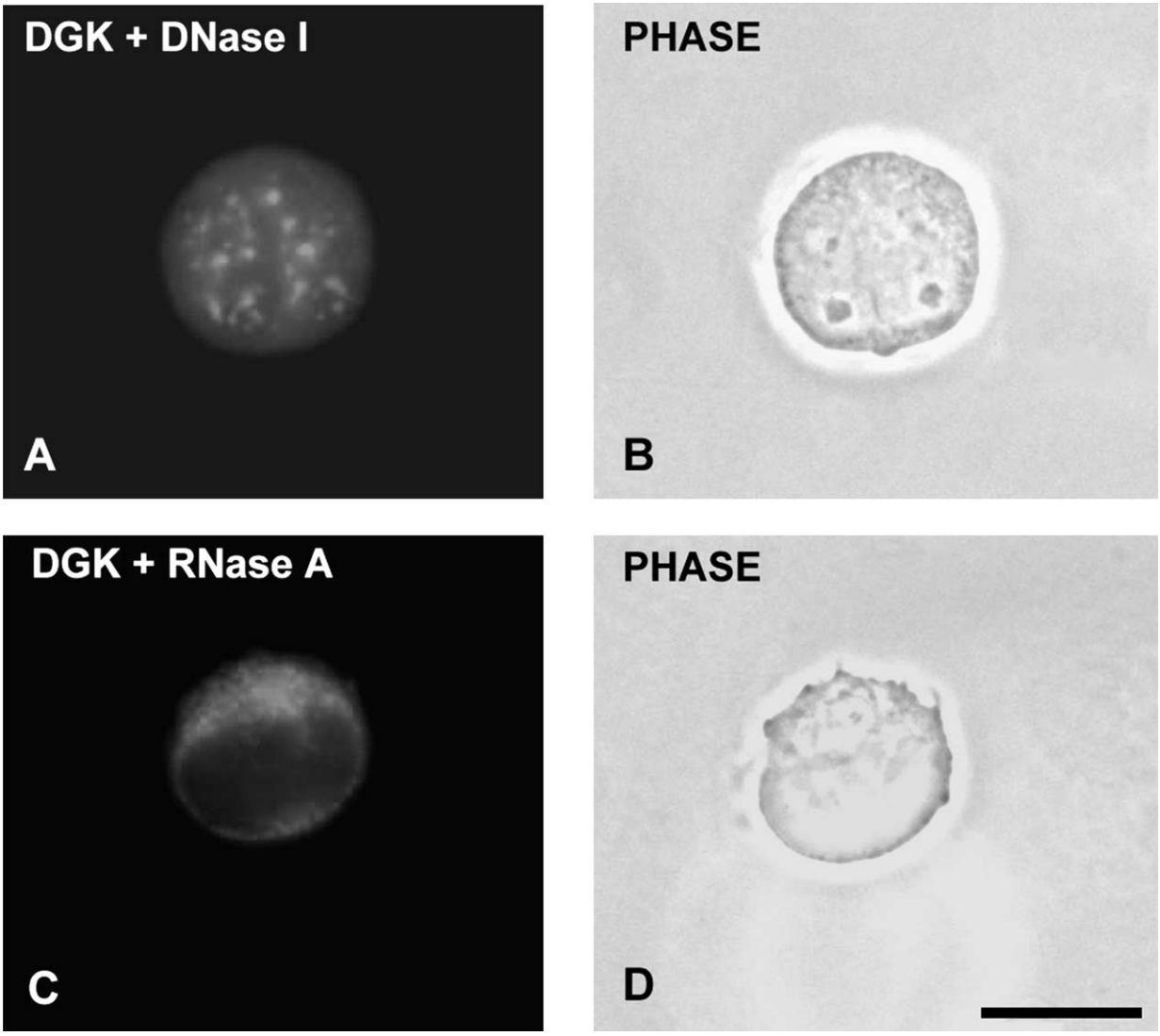

Fig. 4. Nuclease sensitivity of DGK-θ in MDA-MB-453 cells. RNase A (C), but not DNase I (A), treatment abolishes nuclear DGK-θ staining. (B, D) Corresponding phase-contrast images. For these experiments, samples have been photographed with a Zeiss Axiophot epifluorescence microscope. Bar = 5 μm.

Nuclear DGK-θ associates with PLCβ1 and PIPKIα in MDA-MB-453 cells

An immunoprecipitation approach was chosen to define the components associated with DGK-θ in interphase nuclei. MDA-MB-453 cell nuclear extracts were immunoprecipitated with either antibody to PIP_2 or antibody to PLCβ1. As shown in Fig. 8, antibody to PIP_2 immunoprecipitated some of the phosphorylated form of RNA pol II present in the nuclear lysates. The fact that not all of the hyperphosphorylated RNA pol II was immunoprecipitated by antibody to PIP_2 was consistent with the observation that hyperphosphorylated RNA pol II was only partially localized in the speckles [28]. However, anti-PIP_2 antibody immunoprecipitated neither DGK-θ nor PIPKIα, which were recovered in the supernatants of the immunoprecipitates. In contrast, antibody to PLCβ1 failed to immunoprecipitate the hyperphosphorylated form of RNA pol II, but immunoprecipitated a substantial amount of both DGK-θ and PIPKIα originally present in the nuclear lysates.

Discussion

Compelling evidence suggests that nuclear speckles contain some elements of phosphoinositide metabolism [25–27]. In this article, we have clearly demonstrated for the first time that DGK-θ also localizes to the nuclear speckle domains in different cell lines. Such a conclusion derives from several lines of evidence. Immunofluorescence staining coupled to CLSM analysis showed nuclear DGK-θ to be concentrated in discrete structures that, for their number and size, reminded us of nuclear speckles. Double-immunofluorescence staining experiments showed that nuclear DGK-θ and PIP_2 almost completely co-localized. Previous results have demonstrated that PIP_2 is concentrated in nuclear

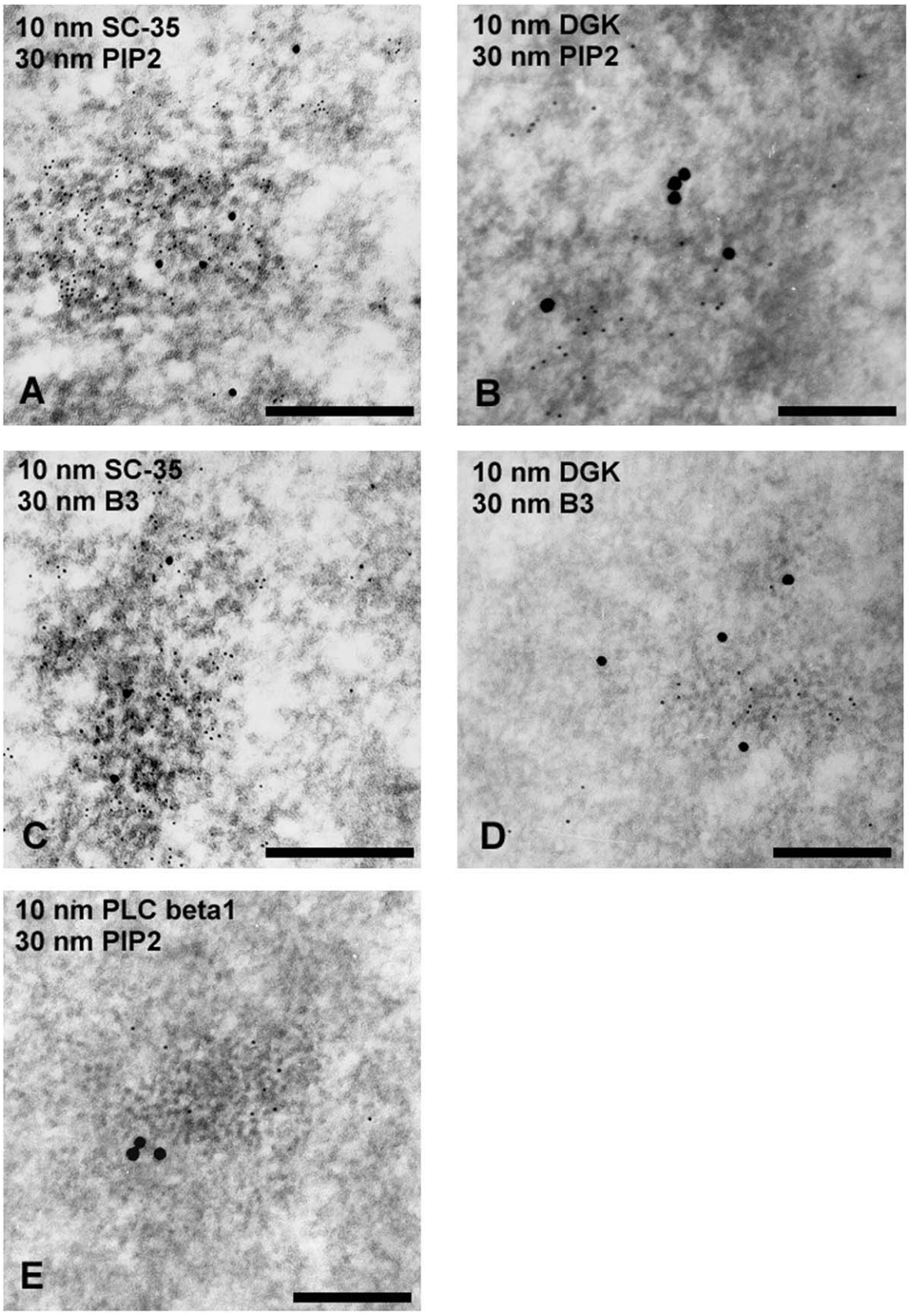

Fig. 5. Immuno-electron microscopy of MDA-MB-453 cells labeled with antibodies to SC-35, PIP_2, DGK-θ, hyperphosphorylated RNA pol II (antibody B3), and PLCβ1. Primary antibodies were mouse IgG (SC-35, DGK-θ, PLCβ1) and IgM (PIP_2, B3). Localization of the antigens was shown by gold colloid particles (either 10 nm to reveal IgG or 30 nm to label IgM) conjugated with the secondary antibody, as indicated in each panel. Bars = 250 nm.

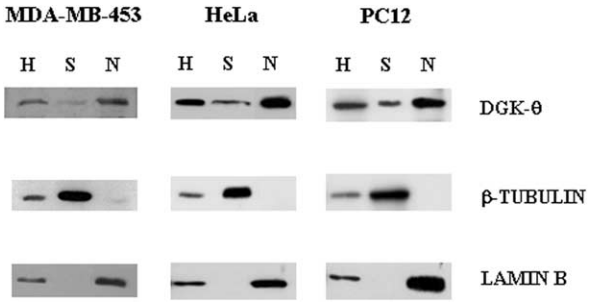

Fig. 6. DGK-θ is enriched in the nuclear fraction. Subcellular fractionation experiments showing the distribution of DGK-θ in various cell lines by Western blot. H, whole-cell homogenate; S, postnuclear supernatant; N, purified nuclei. Note the absence of β-tubulin from nuclear preparations that, on the other hand, were enriched in the nuclear-specific protein lamin B. Eighty micrograms of protein was blotted to each lane.

speckles [25,26]. We have confirmed these findings in MDA-MB-453 cells by showing that the immunofluorescence staining pattern given by a monoclonal antibody highly specific for PIP_2 [26,37,38] is largely superimposable to that given by an antibody that recognizes the splicing component SC-35, a well-recognized marker of nuclear speckles [34]. Moreover, the nuclear DGK-θ fluorescence pattern was sensitive to α-amanitin, a fungal toxin known to affect the number and/or the size of nuclear speckles [33]. Taken together, these data strongly suggested that DGK-θ is located in the nuclear speckles. An interesting observation is that the level of co-localization of PIP_2 with DGK-θ was not completely maintained after treatment with α-amanitin. On the other hand, almost complete co-localization of SC-35 with PIP_2 was detected also in samples treated with the fungal toxin. Even though we could not perform double-immunofluorescence staining for SC-35/DGK-θ due to the lack of a suitable polyclonal antibody to SC-35, our findings seem to indicate that most of the DGK-θ does not co-localize with SC-35 under conditions of impaired mRNA synthesis. This might depend on a different sensitivity and/or behavior of the speckle components to α-amanitin.

Also, immuno-electron microscopy unequivocally showed that, in MDA-MB-453 cells, DGK-θ was present in the interchromatin granules and perichromatin fibrils that, at the ultrastructural level, correspond to nuclear speckles [34]. With this technique we were able to perform a double-immunostaining experiment that showed co-localization of DGK-θ with a hyperphosphorylated form of RNA polymerase II, which is known to be present in the speckles [28]. Furthermore, we have shown by immuno-electron microscopy that both PIP_2 and PLCβ1 localize to this nuclear domain.

Cell fractionation experiments showed DGK-θ to be strongly enriched in nuclei prepared from MDA-MB-453, HeLa, and PC12 cells. These results were consistent with the findings provided by immunofluorescence staining that demonstrated that DGK-θ was preferentially present in the nucleus. DGK-θ was enriched in the nuclear matrix fraction prepared from MDA-MB-453. Even though the DGK-θ enrichment in the nuclear matrix was not as marked as that of 170-kDa DNA topoisomerase IIα, it was nevertheless higher than that of NuMA protein, another constituent of the nuclear matrix. This conceivably depends on the fact that not all DGK-θ is matrix-bound, as also reported for NuMA [39]. DGK-θ which can be recovered associated to the nuclear matrix might represent the active fraction of the enzyme. Indeed, the nuclear matrix is viewed by several investigators as the fundamental organizing principle of the nucleus where many functions take place, including DNA replication, gene expression, and protein phosphorylation [40–42]. Several enzymes of the inositol lipid metabolism have been found associated with the nuclear matrix [reviewed in 8,43], and this indicates that the matrix may also be involved in intranuclear signal transduction pathways.

The presence of DGK in the nucleus was first shown by immunocytochemical staining of rat retina and brain [44]. Following this report, other groups have demonstrated that DGK-ζ [20], -α or -γ [23] and DGK-θ [6] are intranuclear. DAG kinase-ζ possesses a bipartite nuclear targeting motif located close to the second zinc finger-like sequence in its regulatory domain [20]. However, the nuclear localization sequences of other DGK isoforms remain to be identified. In any case, it will also be very important to analyze whether or not DGK-θ displays a sequence element directing it to the speckles, such as the motif recently identified in the essential spliceosomal protein $SF3b^{155}$ [45]. Evidence indicates that DGK-θ was responsible for the increased nuclear DGK activity that followed stimulation of quiescent IIC9 cells with α-thrombin [22]. It should be emphasized that resting IIC9 cells displayed immunoreactivity for DGK-θ both in the cytoplasm and in the nucleus. The nuclear staining pattern given by the same monoclonal antibody to DGK-θ employed in this study was reminiscent of nuclear speckles. However, after stimulation with α-thrombin there was translocation of some DGK-θ from the cytoplasm to the nucleus, as shown by Western blot, but the overall nuclear fluorescence pattern did not change.

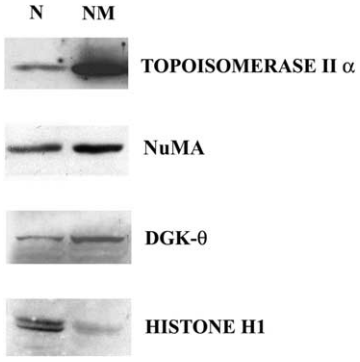

Fig. 7. Nuclear DGK-θ associates with the nuclear matrix prepared from MDA-MB-453 cells. Western blot analysis showing immunoreactivity for 170-kDa topoisomerase IIα, NuMA, DGK-θ, and histone H1 in isolated nuclei (N) and nuclear matrix (NM). Eighty micrograms of protein was blotted to each lane.

Table 3
Densitometric analysis of the Western blots showing association of DGK-θ with the nuclear matrix[a]

Protein	Isolated nuclei	Nuclear matrix	Nuclear matrix/isolated nuclei
170-kDa topoisomerase II α	8.5 ± 1.2	28.9 ± 3.2	3.4
NuMA	14.3 ± 2.2	22.5 ± 2.9	1.6
DGK-θ	6.1 ± 0.9	11.4 ± 1.7	1.9
Histone H1	15.1 ± 2.4	1.7 ± 0.4	0.1

[a] Films were scanned with a Molecular Analyst GS670. Data are expressed in arbitrary units and are representative of three separate experiments ± SD. In the last column, for each protein investigated, we show the fold enrichment in nuclear matrix over isolated nuclei.

The association of DGK-θ with nuclear speckles appears extremely interesting, because of other results showing that several elements of the phosphoinositide cycle are present within this subnuclear compartment. These elements include PIPKIα, PIPKIIα, and PIPKIIβ [25], PIP_2 [25,26], and P13K C2α [27]. By immunoprecipitation we have shown that PIP_2 is associated with a hyperphosphorylated form of RNA pol II, in agreement with others [26]. However, DGK-θ was not recovered in the immunoprecipitates obtained with anti-PIP_2 antibody, but rather in those collected after immunoprecipitation with an antibody to PLCβ1. Interestingly, these immunoprecipitates also contained PIPKIα. This might indicate the existence in the nuclear speckles of a multienzymatic complex composed of proteins involved in phosphoinositide metabolism. PLCβ1 could hydrolyze PIP_2 yielding DAG and inositol 1,4,5-trisphosphate [9,10], while DGK-θ may convert DAG into PA. The presence of PIPKIα (which phosphorylates phosphatidylinositol 4-phosphate to PIP_2) suggests that the speckles are also the site for intranuclear PIP_2 synthesis. The detergent-resistant PIP_2 pool in the speckles has also been related to a role played by this inositol lipid in pre-mRNA splicing [26]. Even though DGK-θ apparently did not associate with hyperphosphorylated RNA pol II, RNase A digestion experiments revealed that RNA was important for determining the association of DGK-θ with the speckles. Such a requirement for the presence of RNA has been reported for other components of the speckles, such as PI3K C2α [27] and protein 4.1 N [46]. However, it may be that this simply reflects the fact that DGK-θ is nuclear matrix-bound, because RNA is very important for the structural integrity of the matrix [40,47].

Taken together our findings demonstrate that nuclear DGK-θ is a component of the speckle domains. The localization of DGK-θ to a specific subnuclear site is an important step toward a better understanding of compartmentalization and function of phosphoinositide nuclear metabolism. In the future, it will be interesting to investigate whether or not other DGK isoforms known to be present in the nucleus associate with the speckles and also to establish the exact role played by these isozymes in the context of this nuclear subregion.

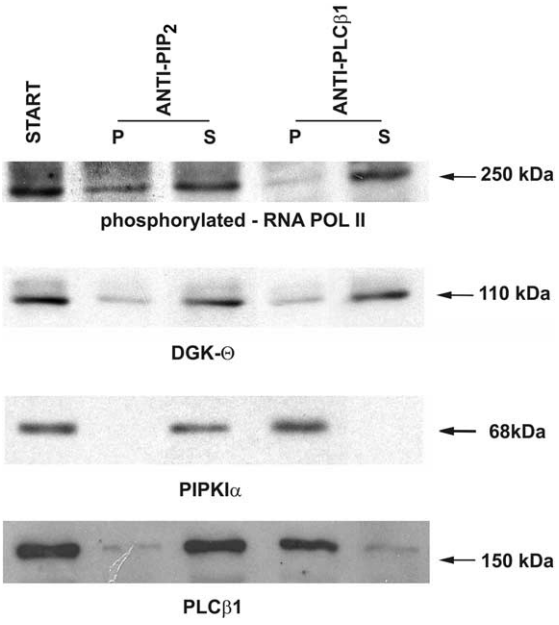

Fig. 8. Nuclear DGK-θ associates with both PLCβ1 and PIPKIα. Samples were analyzed by Western blotting with antibodies against the hyperphosphorylated form of RNA pol II (antibody B3), DGK-θ, or PIPKIα. Start, amount of protein in the nuclear lysates subjected to immunoprecipitation; P, protein recovered in the immunoprecipitates; S, protein in the supernatant from immunoprecipitation.

Acknowledgments

This work was supported by grants from AIRC, Italian MIUR Cofin 2001 and 2002, FIRB 2001, Selected Topics Research Fund from Bologna University, CARISBO Foundation, and by National Institutes of Health Grant GM23922 to R.B.

References

[1] N. Divecha, R.F. Irvine, Phospholipid signalling, Cell 80 (1995) 269–278.
[2] T.E. Martin, Phosphoinositide lipids as signaling molecules: common themes for signal transduction, cytoskeletal regulation, and membrane trafficking, Annu. Rev. Cell Dev. Biol. 14 (1998) 231–264.
[3] M.J.O. Wakelam, Diacylglycerol: when is it an intracellular messenger? Biochim. Biophys. Acta 1436 (1998) 117–126.
[4] D. Ron, M.G. Kazanietz, New insights into the regulation of protein kinase C and novel phorbol ester receptors, FASEB J. 13 (1999) 1658–1676.

[5] W.J. van Blitterswijk, B. Houssa, Properties and functions of diacylglycerol kinases, Cell. Signal. 12 (2000) 595–605.
[6] L. Bregoli, J.J. Baldassare, D.M. Raben, Nuclear diacylglycerol kinase-θ is activated in response to α-thrombin, J. Biol. Chem. 276 (2001) 23288–23295.
[7] C.S. D'Santos, J.H. Clarke, N. Divecha, Phospholipid signalling in the nucleus: Een DAG uit het leven van de inositide signalering in de nucleus, Biochim. Biophys. Acta 1436 (1998) 201–232.
[8] N. Divecha, J.H. Clarke, M. Roefs, J.R. Halstead, C. D'Santos, Nuclear inositides: inconsistent consistencies, Cell. Mol. Life Sci. 57 (2000) 379–393.
[9] L. Cocco, A.M. Martelli, R.S. Gilmour, S.G. Rhee, F.A. Manzoli, Nuclear phospholipase C and signaling, Biochim. Biophys. Acta 1530 (2001) 1–14.
[10] L. Cocco, A.M. Martelli, O. Barnabei, F.A. Manzoli, Nuclear inositol lipid signaling, Adv. Enzyme Regul. 41 (2001) 361–384.
[11] A.M. Martelli, R. Bortul, G. Tabellini, M. Aluigi, D. Peruzzi, R. Bareggi, P. Narducci, L. Cocco, Re-examination of the mechanisms regulating nuclear inositol lipid metabolism, FEBS Lett. 505 (2001) 1–6.
[12] Irvine, R.F. Nuclear lipid signaling. *Science's STKE*, http://www.stke.org/cgi/content/full/sigtrans;2002/150/re13 (2002).
[13] K. Goto, H. Kondo, Diacylglycerol kinase in the central nervous system: molecular heterogeneity and gene expression, Chem. Phys. Lipids 98 (1999) 109–117.
[14] W.J. van Blitterswijk, B. Houssa, Diacylglycerol kinases in signal transduction, Chem. Phys. Lipids 98 (1999) 95–108.
[15] M.K. Topham, S.M. Prescott, Mammalian diacylglycerol kinases, a family of lipid kinases with signaling functions, J. Biol. Chem. 274 (1999) 11447–11450.
[16] W.J. van Blitterswijk, B. Houssa, Properties and functions of diacylglycerol kinases, Cell. Signal. 12 (2000) 595–605.
[17] H. Kanoh, K. Yamada, F. Sakane, Diacylglycerol kinases: emerging downstream regulators in cell signaling systems, J. Biochem. 131 (2002) 629–633.
[18] L.M. Neri, P. Borgatti, S. Capitani, A.M. Martelli, Protein kinase C isoforms and lipid second messengers: a critical nuclear partnership? Histol. Histopathol. 17 (2002) 1311–1316.
[19] A.M. Martelli, R. Bortul, G. Tabellini, R. Bareggi, L. Manzoli, P. Narducci, L. Cocco, Diacylglycerol kinases in nuclear lipid-dependent signal transduction pathways, Cell. Mol. Life Sci. 59 (2002) 1129–1137.
[20] M.K. Topham, M. Bunting, G.A. Zimmerman, T.M. McIntyre, P.J. Blackshear, S.M. Prescott, Protein kinase C regulates the nuclear localization of diacylglycerol kinase-ζ, Nature 394 (1998) 697–700.
[21] A.M. Martelli, G. Tabellini, R. Bortul, L. Manzoli, R. Bareggi, G. Baldini, V. Grill, M. Zweyer, P. Narducci, L. Cocco, Enhanced nuclear diacylglycerol kinase activity in response to a mitogenic stimulation of quiescent Swiss 3T3 cells with insulin-like growth factor-1, Cancer Res. 60 (2000) 815–821.
[22] L. Bregoli, B. Tu-Sekine, D. Raben, DGK and nuclear signaling: nuclear diacylglycerol kinases in IIC9 cells, Adv. Enzyme Regul. 42 (2002) 213–226.
[23] Y. Shirai, S. Segawa, M. Kuriyama, K. Goto, N. Sakai, N. Saito, Subtype-specific translocation of diacylglycerol kinase α and γ and its correlation with protein kinase C, J. Biol. Chem. 275 (2000) 24760–24766.
[24] M. Dundr, T. Misteli, Functional architecture in the cell nucleus, Biochem. J. 356 (2001) 297–310.
[25] I.V. Boronenkov, J.C. Loijens, M. Umeda, R.A. Anderson, Phosphoinositide pathways in nuclei are associated with nuclear speckles containing pre-mRNA processing factors, Mol. Biol. Cell 9 (1998) 3547–3560.
[26] S.L. Osborne, C.L. Thomas, S. Gschmeissner, G. Schiavo, Nuclear PtdIns(4,5)P_2 assembles in a mitotically regulated particle involved in pre-mRNA splicing, J. Cell Sci. 114 (2001) 2501–2511.
[27] S.A. Didichenko, M. Thelen, Phosphatidylinositol 3-kinase C2α contains a nuclear localization sequence and associates with nuclear speckles, J. Biol. Chem. 276 (2001) 48135–48142.
[28] M.J. Mortillaro, B.J. Blencowe, X. Wei, H. Nakayasu, L. Du, S.L. Warren, P.A. Sharp, R. Berezney, A hyperphosphorylated form of the large subunit of RNA polymerase II is associated with splicing complexes and the nuclear matrix, Proc. Natl. Acad. Sci. USA 93 (1996) 8253–8257.
[29] P. Borgatti, M. Mazzoni, C. Carini, L.M. Neri, M. Marchisio, L. Bertolaso, M. Previati, G. Zauli, S. Capitani, Changes of nuclear PKC activity and isotype composition in PC12 cell proliferation and differentiation, Exp. Cell Res. 224 (1996) 72–78.
[30] P. Belgrader, A.J. Siegel, R. Bereznccy, A comprehensive study on the isolation and characterization of the HeLa S3 nuclear matrix, J. Cell Sci. 98 (1991) 281–291.
[31] M. Riccio, R. Di Giamo, S. Pianetti, P.P. Calmieri, M. Melli, S. Santi, Nuclear localization of cystatin B, the cathepsin inhibitor implicated in myoclonus epilepsy (EPM1), Exp. Cell Res. 262 (2001) 84–94.
[32] E.M.M. Manders, F.J. Verbeek, A. Aten, Measurement of co-localization of object in dual-colour confocal images, J. Microsc. 169 (1993) 375–382.
[33] M. Carmo-Fonseca, R. Pepperkok, M.T. Carvalho, A.I. Lamond, Transcription-dependent colocalization of the U1, U2, U4/U6, and U5 snRNPs in coiled bodies, J. Cell Biol. 117 (1992) 1–14.
[34] D.L. Spector, X.D. Fu, T. Maniatis, Associations between distinct pre-mRNA splicing components and the cell nucleus, EMBO J. 10 (1991) 4367–3481.
[35] M. Berrios, N. Osheroff, P.A. Fisher, In situ localization of DNA topoisomerase II, a major polypeptide component of the *Drosophila* nuclear matrix, Proc. Natl. Acad. Sci. USA 82 (1985) 4142–4146.
[36] P. Barboro, C. D'Arrigo, M. Mormino, R. Coradeghini, S. Parodi, E. Patrone, C. Balbi, An intranuclear frame for chromatin compartmentalization and higher-order folding, J. Cell. Biochem. 88 (2003) 113–120.
[37] G.D. Prestwich, R. Chen, L. Feng, S. Ozaki, C.G. Ferguson, B.E. Drees, D.A. Neklason, C.G. Mostert, P.A. Porter-Gill, V.H. Kang, J.C. Shope, P.O. Neilsen, D.B. Dewald, In situ detection of phospholipid and phosphoinositide metabolism, Adv. Enzyme Regul. 42 (2002) 19–38.
[38] R. Chen, V.H. Kang, J. Chen, J.C. Shope, J. Torabinejad, D.B. DeWald, G.D. Prestwich, A monoclonal antibody to visualize PtdIns(3,4,5)P_3 in cells, J. Histochem. Cytochem. 50 (2002) 697–708.
[39] C. Zeng, D. He, S.M. Berget, B.R. Brinkley, Nuclear-mitotic apparatus protein: a structural protein interface between the nucleoskeleton and RNA splicing, Proc. Natl. Acad. Sci. USA 91 (1994) 1505–1509.
[40] J.A. Nickerson, Experimental observations of a nuclear matrix, J. Cell Sci. 114 (2001) 463–474.
[41] R. Berezney, Regulating the mammalian genome: the role of nuclear architecture, Adv. Enzyme Regul. 42 (2002) 39–52.
[42] A.M. Martelli, E. Falcieri, M. Zweyer, R. Bortul, G. Tabellini, A. Cappellini, L. Cocco, L. Manzoli, The controversial nuclear matrix: a balanced point of view, Histol. Histopathol. 17 (2002) 1193–1205.
[43] N.M. Maraldi, N. Zini, S. Santi, F.A. Manzoli, Topology of inositol lipid signal transduction in the nucleus, J. Cell. Physiol. 181 (1999) 203–217.
[44] K. Goto, H. Kondo, A 104-kDa diacylglycerol kinase containing ankyrin-like repeats localizes in the cell nucleus, Proc. Natl. Acad. Sci. USA 93 (1996) 11196–11201.
[45] J. Eilbracht, M.S. Schmidt-Zachmann, Identification of a sequence element directing a protein to nuclear speckles, Proc. Natl. Acad. Sci. USA 98 (2001) 3849–3854.
[46] M.-J. Lallena, I. Correas, Transcription-dependent redistribution of nuclear protein 4.1 to SC35-enriched nuclear domains, J. Cell Sci. 110 (1997) 239–247.
[47] P. Barboro, C. D'Arrigo, A. Diaspro, M. Formino, I. Alberti, S. Parodi, E. Patrone, C. Balbi, Unraveling the organization of the internal nuclear matrix: RNA-dependent anchoring of NuMa to a lamin scaffold, Exp. Cell Res. 279 (2002) 2002–2018.